

Conodont biostratigraphy and biofacies across the Devonian-Carboniferous boundary in the Kule section (Uzbekistan)

Katarzyna NARKIEWICZ^{1,*}, Carlo CORRADINI², Nuriddin ABDIEV³
and Marek NARKIEWICZ¹

- ¹ Polish Geological Institute – National Research Institute, Rakowiecka 4, 00-975 Warszawa, Poland
- ² Università di Trieste, Dipartimento di Matematica e Geoscienze, via Weiss 2, 34128 Trieste, Italy
- ³ Kitab State Geological National Natural Park, Kashkadarya Region, Kitab District, Ipak Yuli Street 9, 181300 Shakhrisabz, Uzbekistan



Narkiewicz, K., Corradini, C., Abdiev, N., Narkiewicz, M., 2021. Conodont biostratigraphy and biofacies across the Devonian-Carboniferous boundary in the Kule section (Uzbekistan). *Geological Quarterly*, 2021, 65: 17, doi: 10.7306/gq.1588

Associate Editor: Michał Zatoń

New conodont data provide further constraints on the occurrence of the Devonian-Carboniferous boundary in the Kule section through the carbonate Novchomok Formation (Kitab Reserve, Uzbekistan). The stratigraphically condensed section includes the interval from the uppermost Famennian *Pseudopolygnathus granulatus*–lowermost *Protognathodus kockeli* zones to the middle Tournaisian *Siphonodella crenulata* Zone. In addition to revision of earlier published taxonomic and biostratigraphic data, two previously unreported taxa are described: *Polygnathus* sp. n. A and a peculiar form probably representing a new genus (gen. et sp. indet.). The biofacies analysis documents a succession of polygnathid, siphonodellid-polygnathid, polygnathid-siphonodellid to polygnathid-bispathodid, and again polygnathid-siphonodellid biofacies. The generic composition of the samples and relative abundance of *Polygnathus purus* reflect deep marine environments of the continental slope and rise.

Key words: DCB, carbonate facies, conodont biostratigraphy, biofacies analysis, deep marine environment.

INTRODUCTION

The Devonian-Carboniferous boundary (DCB) is the subject of continuing research focused on unresolved biostratigraphic problems (i.a. Flais and Feist, 1988; Ziegler and Sandberg, 1996; Kaiser, 2009; Kaiser and Corradini, 2011; Corradini et al., 2011, 2017b, 2020). Much study is also being devoted to global events connected with this boundary, the Hangenberg Event in particular (Kaiser et al., 2009, 2016; Marynowski et al., 2012; Matyja et al., 2015; Becker et al., 2016; Kumpan et al., 2019; Paschall et al., 2019; Rakociński et al., 2020; Shizuya et al., 2020). With regard to these issues, the Kule section in Uzbekistan has been a focus of the working group established in 2008 by the International Commission on Stratigraphy to redefine the boundary and find a new GSSP (Global Boundary Stratotype Section and Point). The results of

early conodont investigations of the section, suggesting the possibility of documenting the DCB, were given during a joint meeting of the Subcommittee on Devonian Stratigraphy and IGCP Project 499 (Yolkin et al., 2008: p. 46; Kim et al., 2008). The locality was inspected and resampled by participants of the excursion organized during the meeting (Matyja, 2011). Thereafter, it was measured and sampled in 2015 by a field party from the Silesian University in Sosnowiec (Dubicka and Rakociński, 2015, unpubl. report). The present study, based on the results of the latter fieldwork, supplied new conodont data which allowed updating of the earlier findings (Erina, 2008a, b). Preliminary data and interpretations were presented during the 4th International Conodont Symposium in Valencia (Narkiewicz et al., 2017). This paper reports new taxonomic, biostratigraphic and biofacies results from the interval spanning the DCB and the lower Tournaisian (lowermost Mississippian) strata.

REGIONAL AND STRATIGRAPHIC SETTING

The Kule section is located in the Kitab Reserve Area in SE Uzbekistan, in the Zeravshan-Gissar Mountains of the SW Tian Shan, not far from the Pragian-Emsian GSSP in the Zinzil'ban

* Corresponding author, e-mail: katarzyna.narkiewicz@pgi.gov.pl
Received: December 17, 2020; accepted: February 4, 2021;
accepted: first published online: 1 April, 2021

Gorge (Yolkin et al., 1997; Fig. 1). The exposures occupy the southern flank of the Dzhindy-Darya River near the eastern margin of the Kitab Natural Park (Yolkin et al., 2008: p. 68).

The section studied is a part of folded and faulted Middle Devonian to Lower Carboniferous succession exposed along the left slope of the Kule Gorge (Yolkin et al., 2008: fig. 15). The interval investigated corresponds to a part of the Novchomok Formation, the unit comprising the local uppermost Famennian and Tournaisian (Yolkin et al., 2008: p. 68). The formation is developed as grey and light grey, variably bedded, partly massive limestones (Figs. 2 and 3). The deposits are fine-grained and micritic, in places brecciated, bioclastic, with irregular bedding surfaces. They contain crinoids, rare brachiopods and coral fragments. According to an earlier study (Yolkin et al., 2008: fig. 14), the DCB interval, from an undifferentiated *praesulcata* to the *crenulata* zones, is only 15 m thick, which suggests some degree of stratigraphic condensation.

tained is 250 and their preservation state is moderately good to poor. Most specimens are broken, fractured and in some cases the upper ornamented surface has been scraped off, probably due to tectonic fracturing and shearing.

The conodont abundance in the samples, summarised in Table 1, is mostly 20–40 specimens per sample, except for sample 5B, where the abundance reaches about one hundred. The conodont assemblages contain elements of different ontogenetic stages, from early juvenile to mature. This indicates insignificant post-mortem, hydrodynamic, sorting which in turn suggests the occurrence of *in situ* assemblages (see the section on biofacies below). The colour alteration index (CAI) of mature specimens is 3, corresponding to palaeotemperatures 110–200°C (Epstein et al., 1977).

Conodonts described herein are stored at the Silesian University in Sosnowiec, Poland.

MATERIAL STUDIED

Altogether, 37 samples were taken in 2015 by Dubicka and Rakociński from the Kule section, out of which seven were analysed in this study (Fig. 2). The samples, the weight of which varied between 0.25 and 0.55 kg, were dissolved in 15% formic acid and the heavy residue with conodonts was separated using sodium metatungstate. The total number of specimens ob-

BIOSTRATIGRAPHY

Table 1 summarises the conodont taxa found in the samples, their frequency and the biostratigraphy of the microfossil assemblages. The conodont biostratigraphy is based on the literature data cited below, and is discussed in stratigraphic order. In addition, the stratigraphic ranges attributed to particular samples are visualised with reference to the conodont zonation of the uppermost Devonian-lowermost Carboniferous (Fig. 4).

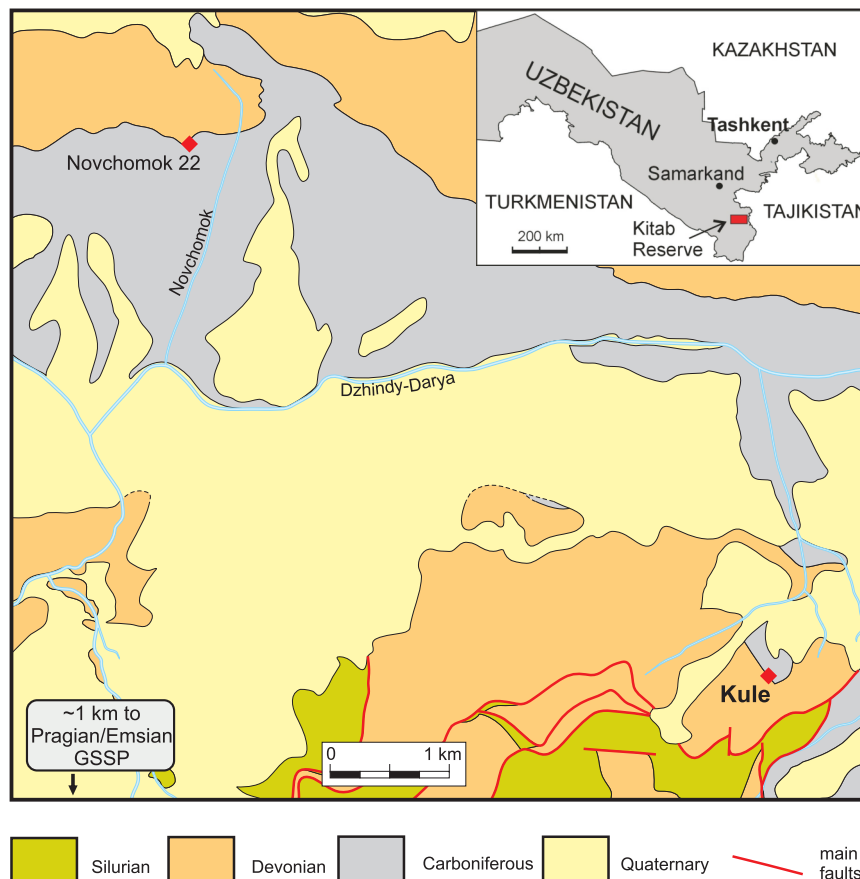
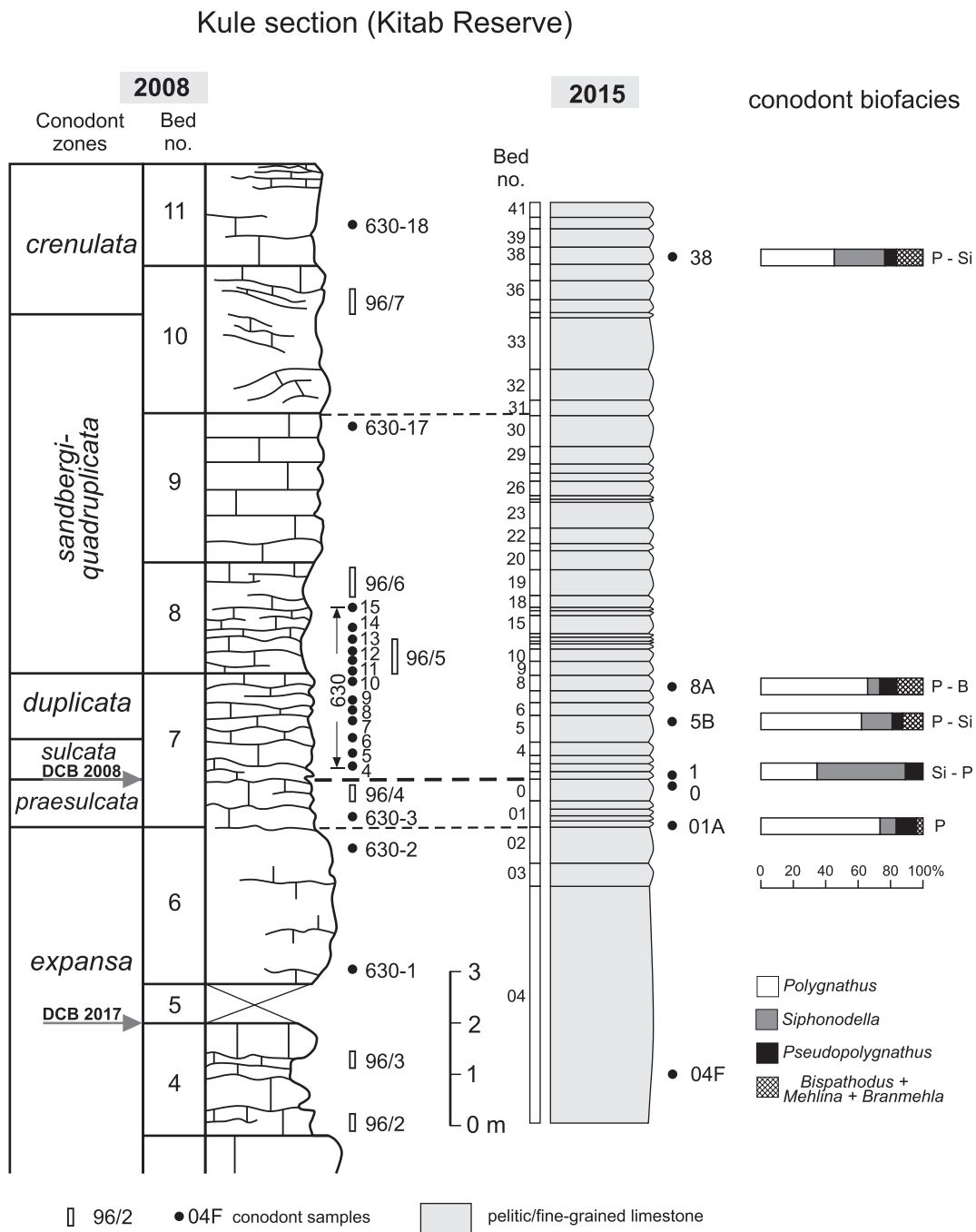


Fig. 1. Geological sketch-map showing the location of the section investigated, the inset map of Uzbekistan showing the location of the Kitab Reserve



DCB 2008 - Devonian-Carboniferous boundary according to the Guidebook (2008)

DCB 2017 - Devonian-Carboniferous boundary according to Erina *vide* Salimova (2017, pers. comm.)

Fig. 2. Location of the samples investigated and corresponding conodont biofacies (right) against the relevant part of the Novchomok Formation in the Kule section (Dubicka and Rakociński, 2015, unpubl. report) compared with the equivalent part (left) of the section published in Yolkin et al. (2008: fig. 14)

The biostratigraphic correlation of the two columns is discussed in the text; abbreviations: P – polygnathid, Si – siphonodellid, B – bispathodid (*Bispathodus*, *Mehlina*, *Branmehla*)

The taxa important for stratigraphy and interesting from a taxonomic viewpoint are illustrated in Figures 5–8.

Various conodont zonation schemes are applied across the DCB. The classical subdivisions by Ziegler and Sandberg (1990) for the Upper Devonian and Sandberg et al. (1978) for

the Tournaisian have been updated by Corradini (2008), Kaiser et al. (2009), and Spalletta et al. (2017). Also, due to difficulties in recognizing the early siphonodellids, a new zonation across the DCB was introduced by Corradini et al. (2017b). This scheme is less detailed than the previous one for the uppermost



Fig. 3. Field photo showing the DCB position according to the concept of [Yolkin et al. \(2008: fig. 14\)](#)

Photo by M. Rakociński taken in 2015

Famennian interval, as the *Bispathodus ultimus* Zone includes the previous Upper *expansa*, Lower and Middle *praesulcata* zones. Therefore, [Corradini et al. \(2020\)](#) introduced in the upper part of the *Bi. ultimus* Zone the *Protognathodus meischneri* Subzone, the base of which is approximately equivalent to the base of the former Lower *praesulcata* Zone of [Ziegler and Sandberg \(1990\)](#) and of the *Siphonodella praesulcata* Zone of [Kaiser et al. \(2009\)](#). In this paper we apply the most recent zonation ([Spalletta et al., 2017; Corradini et al., 2020](#)), with the modification suggested by [Becker et al. \(2016\)](#) to rename the *Siphonodella hassi* Zone as that of *Siphonodella jii*, due to taxonomic problems with the index species.

The biostratigraphic position of the sample 04F assemblage is defined by the total stratigraphic range of *Palmatolepis gracilis sigmoidalis* ([Fig. 6A, B](#)), that is, from the middle part of the *Pseudopolygnathus granulosus* Zone to lowermost part of the *Protognathodus kockeli* Zone ([Spalletta et al., 2017, 2020](#)). The presence of *Pa. gracilis sigmoidalis* above the Hangenberg Black Shale Event has been often considered by German authors as a result of reworking from older sediments (e.g., [Kaiser et al., 2009](#)). It is documented, however, in the lower part of the *Pr. kockeli* Zone in sections where there is no sedimentation break and the sequence is continuously carbonate without any

evidence of reworking (e.g., Grüne Schneid, Sentiero Cresta Verde; [Spalletta et al., 2020](#)).

The stratigraphically important species in the sample 01A is *Siphonodella sulcata* ([Fig. 5J, K](#)), the present marker for the base of the Carboniferous, the first appearance of which indicates the base of the eponymous zone. The upper biozonal limit is set by the biostratigraphy of the assemblage from sample 1 higher in the section (see below) and thus sample 01A is referred to an interval from the upper part of the *Pr. kockeli* Zone (*sulcata/kuehni* Zone of [Kaiser et al., 2009](#)) into the *Siphonodella duplicata* Zone.

Sample 0 did not yield any characteristic conodonts. The lack of *Si. jii* (which appears higher in the section) may point to an age older than the *Si. jii* Chron.

Samples 1 and 5B are attributed to the *Siphonodella jii* Zone based on the presence of representatives of *Si. jii* in both samples (respectively: [Fig. 5V, W, X–Z](#)) and specimens attributed to *Polygnathus* cf. *P. tenuiserratus* ([Fig. 7F, G](#)) found in the higher sample. *Siphonodella jii* is the index species for this zone ([Becker et al., 2016](#)), whereas *Po. tenuiserratus* has been found so far only in Sardinia in the interval comprising the *Siphonodella bransonii* to the *Si. jii* zones ([Corradini et al., 2003, 2020; Mossoni et al., 2015](#)). Other characteristic species found in both samples are *Si. sulcata* ([Fig. 5H, J](#)) and *Si. duplicata* Morphotype 3 ([Fig. 5R–U; see Ji and Ziegler, 1993](#)).

Sample 8A has an impoverished fauna compared to the previous sample, and does not include any stratigraphically diagnostic taxa. *Pseudopolygnathus multistriatus* ([Fig. 8P–R](#)) and a juvenile stage of *Ps. fusiformis* ([Fig. 8V, W](#)) have their last occurrence within the *Si. crenulata* Zone ([Ji and Ziegler, 1993](#)). Consequently, the assemblage from sample 8A is attributed to the *Si. jii–Si. crenulata* interval.

The position of sample 38 against the conodont zonation is determined by the co-occurrence of *Siphonodella* cf. *Si. isosticha* ([Fig. 6C–G](#)), and *Pinacognathus profunda* ([Fig. 6M, N](#)). *Siphonodella isosticha* is reported from the base of the *Si. crenulata* Zone ([Klapper, 1971; Ji and Ziegler, 1993: p. 13; Hogancamp et al., 2019](#)), and *Pi. profunda* has its last occurrence within this zone (e.g., [Klapper, 1966](#)). In sample 38 a single specimen of *Ps. micropunctatus* ([Fig. 8X–Z](#)) has been determined. However, this is a Famennian taxon with its LAD ascribed to the lower part of the *Bi. ultimus* Zone ([Hartenfels, 2011; Corradini et al., 2017; Spalletta et al., 2017](#)). This unusual discovery is probably an artifact of sample processing, otherwise it is difficult to explain, as there is no evidence of reworking in the section studied.

BIOFACIES

Several conodont biofacies models have been proposed for the lower Tournaisian (e.g., [Dreesen et al., 1986; Dreesen, 1992; Kalvoda et al., 1999, 2015; Kaiser et al., 2009, 2017](#)). They demonstrate that the Hangenberg Event and associated extinction of palmatolepids was followed by a proliferation of two surviving genera, *Polygnathus* and *Siphonodella*, which dominated early Tournaisian deep-water environments. Migration paths of the genera, and global and local environmental changes, including eustatic fluctuations, controlled the proportion of both taxa in conodont assemblages. In the lower part of the Tournaisian corresponding to the middle part of the *Pr. kockeli* Zone (= lower and middle part of the *sulcata/kuehni* Zone according to [Kaiser et al., 2009; cf. Fig. 4](#)) the protognathodid-polygnathid biofacies has been observed. This biofacies grades in the upper part of the zone into the polygnathid

Table 1

Taxonomic composition of conodont assemblages and their biostratigraphy in particular samples

Conodont zones	<i>Ps. granul.–Pr. kockeli</i>		<i>Pr. kockeli – Si. duplicata</i>		<i>Siphonodella jii</i>		<i>Si. jii–Si. cren.</i>	<i>Si. cren.</i>
	04F	01A	0	1	5B	8A	38	
Sample numbers	04F	01A	0	1	5B	8A	38	
Weight of samples (kg)	0.47	0.55	0.33	0.25	0.37	0.30	0.43	
<i>Palmatolepis gracilis sigmoidalis</i>	2							
<i>Branmehla inornata</i>					1	5	4	
<i>Branmehla</i> cf. <i>B. inornata</i>	1				1			
<i>Branmehla</i> sp.	2							
<i>Polygnathus purus purus</i>		15	11	4	24	10	8	
<i>Polygnathus</i> cf. <i>P. purus purus</i>		4	3	3	15	2	4	
<i>Pseudopolygnathus primus</i>		1		1				
<i>Pseudopolygnathus</i> cf. <i>P. primus</i>		1	1	1				
<i>Pseudopolygnathus fusiformis</i>						1		
<i>Siphonodella sulcata</i>		1		2	2			
<i>Siphonodella</i> cf. <i>sulcata</i>				1				
<i>Siphonodella</i> sp. (<i>praesulcata</i> → <i>sulcata</i>)				4	2	2		
<i>Siphonodella bransonii</i> → <i>duplicata</i>				1				
<i>Siphonodella duplicata</i> Morphotype 3				1	2			
<i>Siphonodella jii</i>				1	1			
<i>Pseudopolygnathus multistriatus</i>				1		1		
<i>Polygnathus</i> n.sp. A				2	4	1		
<i>Pinacognathus profunda</i>				1			1	
genus and species indet.				1				
<i>Bispathodus</i> cf. <i>B. stabilis</i>					2			
<i>Bispathodus stabilis stabilis</i>					1		1	
<i>Mehlina</i> sp.					5			
<i>Protognathodus</i> sp.					1			
<i>Polygnathus pupus</i> sensu Bardashev 2004: pl. 12, figs. 12, 13					1			
<i>Polygnathus communis carinus</i>					2			
<i>Polygnathus</i> cf. <i>P. tenuiserratus</i>					2			
<i>Polygnathus</i> aff. <i>P. spicatus</i>					1			
<i>Polygnathus</i> aff. <i>P. mehli</i>							1	
<i>Pseudopolygnathus</i> cf. <i>Ps. micropunctatus</i>							1	
<i>Siphonodella cooperi</i>							2	
<i>Siphonodella lobata</i>							1	
<i>Siphonodella</i> cf. <i>Si. isosticha</i>							1	
<i>Siphonodella</i> sp.		2	1	6	11		8	
<i>Pseudopolygnathus</i> sp.		2		1	7	1	2	
<i>Bispathodus</i> sp.		1			2			
<i>Polygnathus</i> sp.	1	3	4		11	7	4	
Ramiforms	3	6	3	2	23	9	6	
Total of P ₁ elements	6	30	20	31	98	30	38	

Ps. granul. – *Pseudopolygnathus granulatus*, *Pr.* – *Protognathodus*, *Si.* – *Siphonodella*, *cren.* – *crenulata*

biofacies. A distinct increase in the proportion of siphonodellids, accompanied by their taxonomic diversification, takes place from the *Si. duplicata* Zone upwards (Souquet et al., 2020). The *Si. jii* to *Si. crenulata* zonal interval is characterized by the polygnathid-siphonodellid or siphonodellid-polygnathid biofacies (Kaiser et al., 2009, 2017; Kalvoda et al., 2015).

The quantitative evaluation of the biofacies succession in the Kule section is possible owing to the sufficient conodont

abundance exceeding 30 specimens in the samples 01A, 1, 5B, 8A, 38 (Table 1). The presence of representatives of various ontogenetic stages, including juvenile and early-juvenile specimens (44%), attests to the autochthonous nature of the assemblages, thus supporting the reliability of the biofacies analysis. This conclusion could be challenged taking into account underrepresentation of ramiform elements relative to platform ones. The delicate ramiforms, however, can be more easily

Chrono-stratigraphy	Conodont zonation		Stratigraphic position of investigated conodont assemblages
	Ziegler and Sandberg (1990) Kaiser et al. (2009) *Becker et al. (2016)	Spalletta et al. (2017) Corradini et al. (2020)	
M.T. (lower part)	<i>crenulata</i>		
LOWER TOURNAISIAN	<i>quadruplicata</i>		
	<i>sandbergi</i>		
	<i>jii*</i>	<i>Siphonodella jii</i>	
	<i>duplicata</i>	<i>Siphonodella duplicata</i>	
	<i>bransoni</i>	<i>Siphonodella bransoni</i>	
	<i>sulcata/kuehni</i>	<i>Protognathodus kockeli</i>	
FAMENNIAN (upper part)	<i>kockeli</i>		
	<i>cost.-kock. interregnum</i>		
	<i>praesulcata</i>	<i>Bispathodus ultimus</i>	
	Upper <i>expansa</i>		
	Middle <i>expansa</i>	<i>Bispathodus costatus</i>	
		<i>Bispathodus ac. aculeatus</i>	
	Lower <i>expansa</i>	<i>Palmatolepis gracilis expansa</i>	
	Upper <i>postera</i>	<i>Palmatolepis gracilis manca</i>	
	Lower <i>postera</i>	<i>Polygnathus styriacus</i>	
	Upper <i>trachytera</i>	<i>Pseudopolygnathus granulosus</i>	
Lower <i>trachytera</i>	<i>Palmatolepis rugosa trachytera</i>		

Fig. 4. Stratigraphic position of the microfossil assemblages investigated relative to conodont zonation schemes of the upper Famennian to lower Tournaisian

MT – middle Tournaisian

fragmented and removed during preparation of samples than the more robust platform individuals. In addition, their hydrodynamic properties could have led to their larger susceptibility to lateral transportation in a water column, even under a weak current regime, and particularly at greater water-depths (Broadhead et al., 1990).

The results of the quantitative biofacies analysis are summarised in Figure 2. The analysis has been conducted following the procedure applied by Sandberg (1976, 1988) and Bultynck

et al. (1998). Individual representatives of the genera *Pinacognathus*, *Protognathodus* and genus indet. have been neglected in calculating respective percentages.

The assemblage from sample 01A corresponds to the polygnathid biofacies with the *Polygnathus* percentage as high as 73% while *Pseudopolygnathus* represents 13% and *Siphonodella* 10% (see Fig. 2). Higher in the section, in sample 1, the assemblage investigated is ascribed to the siphonodellid-polygnathid biofacies. *Siphonodella*, displaying increased

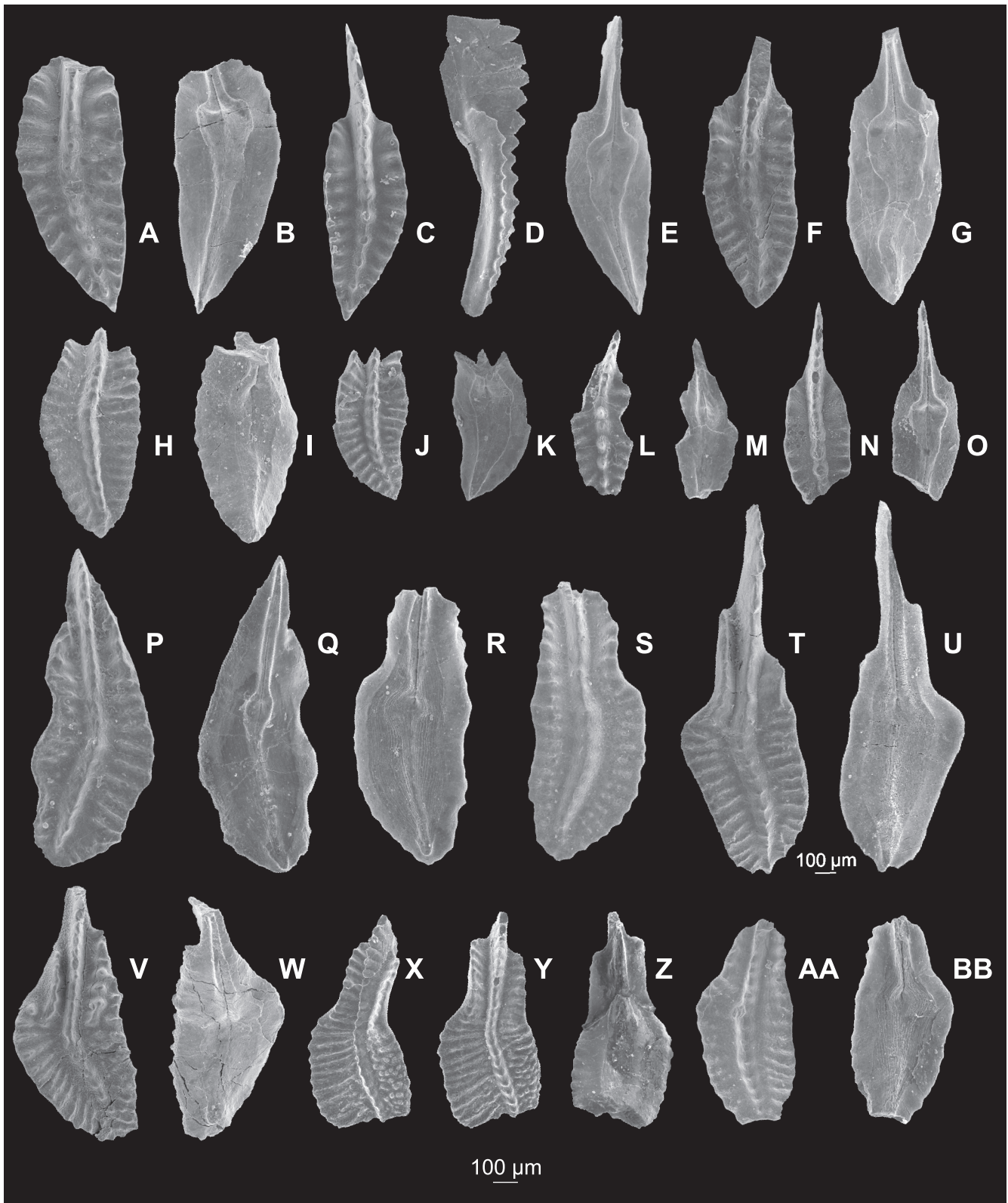


Fig. 5. Selected conodont elements (P_1) of the genus *Siphonodella* from the Kule section

A–G, N, O – *Siphonodella* sp. (transitional forms *praesulcata*→*sulcata*): A, B – upper and lower views, sample 1; F–G – upper and lower views, sample 5B; H–K – *Siphonodella sulcata* (Huddle, 1934): H, I – upper and lower views, sample 5B; J, K – upper and lower views, sample 01A; L, M – *Siphonodella* sp.: L, M – upper and lower views, sample 38; P, Q – *Siphonodella bransonii* Jii, 1985 → *Siphonodella duplicata* (Branson and Mehl, 1934a): P, Q – upper and lower views, sample 1; R–U, AA, BB – *Siphonodella duplicata* (Branson and Mehl, 1934) Morphotype 3 of Ji and Ziegler, 1993: R, S – lower and upper views, sample 5B, T–U – upper and lower views, sample 1, AA, BB – upper and lower views, sample 5B; V–Z – *Siphonodella jii* (Ji, 1985): V, W – upper and lower views, sample 1, X–Z – oblique, upper and lower views, sample 5B; scale bar in all specimens represents 100 μ

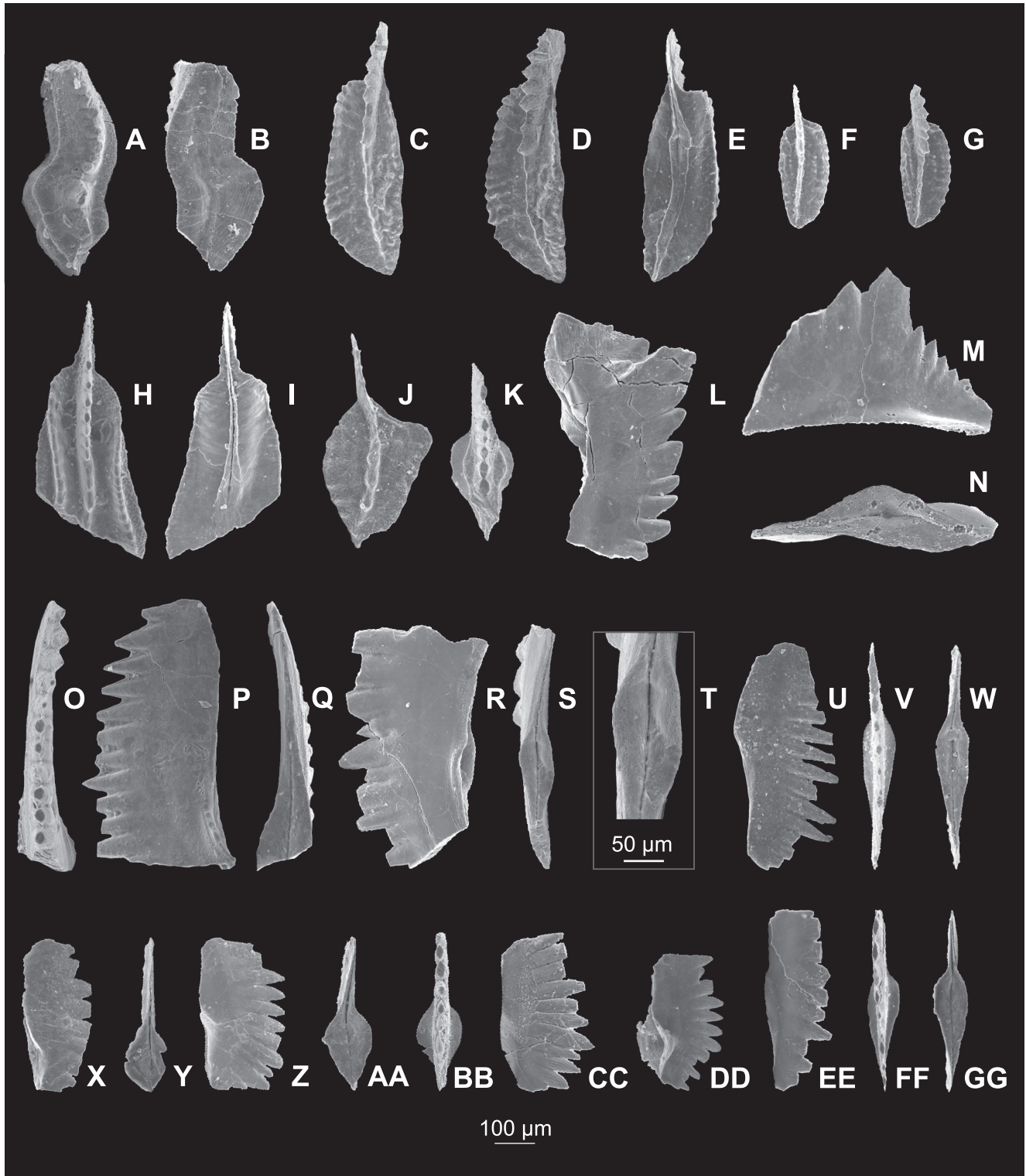


Fig. 6. Selected conodont elements (P_1) from the Kule section

A, B – *Palmatolepis gracilis sigmoidalis* Ziegler, 1962: A, B – upper and lower views, sample 04F; **C–G** – *Siphonodella cooperi* Hass, 1959 M1, sample 38: C–E – upper, oblique and lower views, F, G – upper and upper/oblique views of a juvenile stage; **H, I** – *Siphonodella* cf. *Si. isosticha* (Cooper, 1939): H, I – upper and lower views, sample 38; **J** – *Siphonodella lobata* (Branson and Mehl, 1934a), upper view, sample 38; **K** – *Protognathodus* sp., upper view of a juvenile form, sample 5B; **L–N** – *Pinacognathus profunda* (Branson and Mehl, 1934a): L – lateral view, sample 1, M, N – lateral and lower views, sample 38; **O–Q, EE–GG** – *Bispathodus* cf. *Bi. stabilis* (Branson and Mehl, 1934b): O–Q – upper, lateral and lower views, sample 5B; EE–GG – lateral, upper and lower views, sample 38; **R–W** – *Mehlina* sp., sample 1: R–T – lateral, lower views and enlargement of the pit; U–W – lateral, upper and lower views; **X, Y** – *Branmehla* cf. *Br. inornata* (Branson and Mehl, 1934b): X, Y – lateral and lower views, sample 04F; **Z–DD** – *Branmehla inornata* (Branson and Mehl, 1934b): Z, AA – lateral and lower views, sample 5B, BB, CC – upper and lateral views, sample 8A, DD – lateral/oblique view, sample 38; scale bar in all specimens represents 100 μ

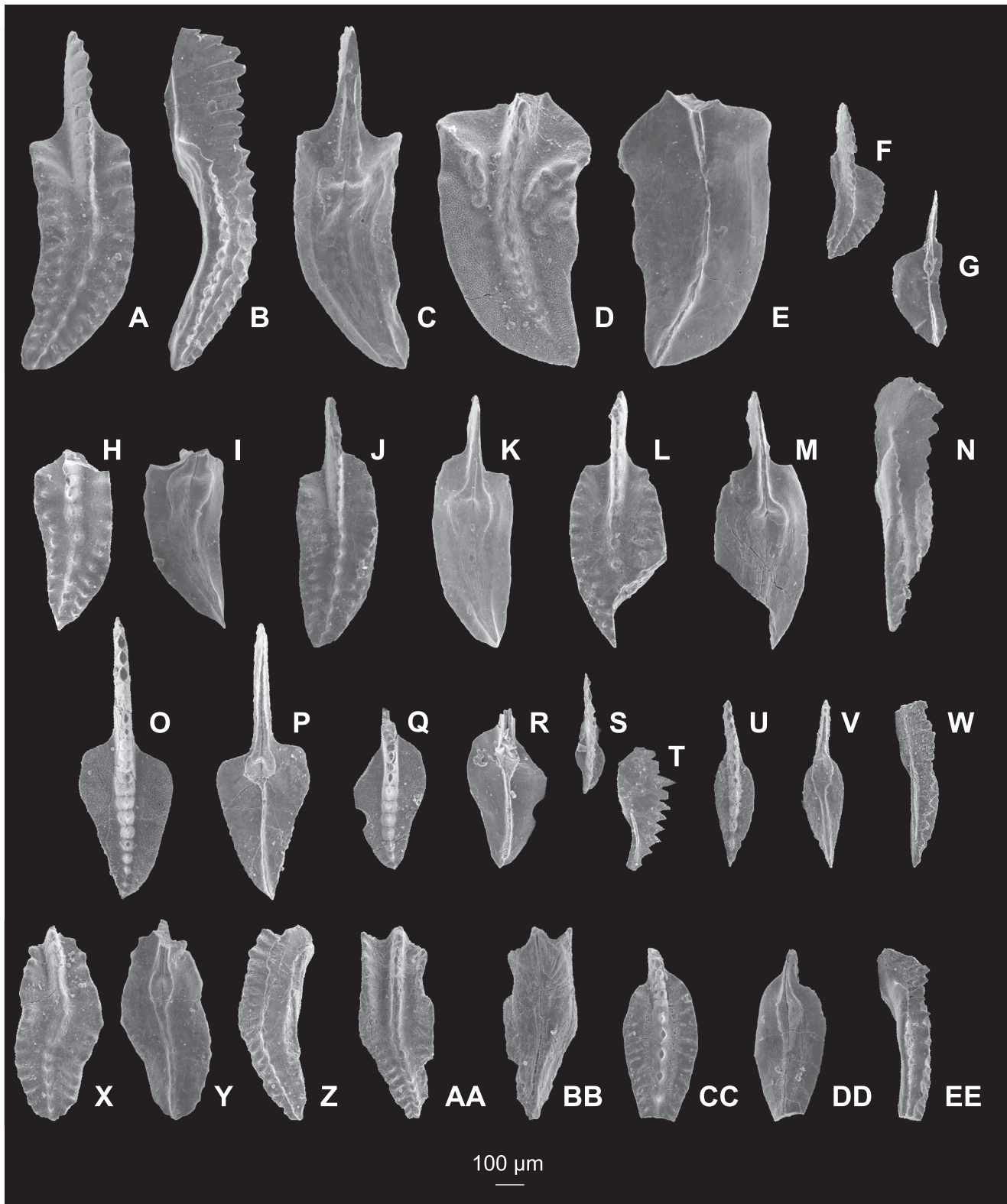


Fig. 7. Selected conodont elements (P_1) of genus *Polygnathus* from the Kule section

A–C, H–N – *Polygnathus* n. sp. A: A–C – upper, lateral and lower views, sample 5B, H–I – upper and lower views of juvenile stage, sample 5B, J, K – upper and lower views, sample 1, L–N – upper, lower and lateral views, sample 1; D, E – *Polygnathus communis carinus* Hass, 1959: D–E – upper and lower views, sample 5B; F, G – *Polygnathus* cf. *P. tenuiserratus* Morphotype 2 Corradini and Spalletta, 2003 (in Corradini et al., 2003): F, G – upper and lower views, sample 5B; O–T – *Polygnathus purus purus* Voges, 1959: O, P – upper and lower views, sample 01A, Q, R – upper and lower views, sample 38, S, T – upper and lateral views of early juvenile stage, sample 01A; U–W – *Polygnathus* sp.: U–W – upper, lower and lateral views, sample 8A; X, Y – *Polygnathus pupus* sensu Bardashev et al. 2004: pl. 12, fig. 12, 13: X, Y – upper and lower views, sample 5B; Z–BB – *Polygnathus* aff. *P. spicatus* Branson, 1934: Z–BB – oblique, upper and lower views, sample 5B; CC–EE – *Polygnathus* aff. *P. mehli* Thompson, 1967: CC–EE – upper, lower and lateral views, sample 38; scale bar in all specimens represents 100 μ

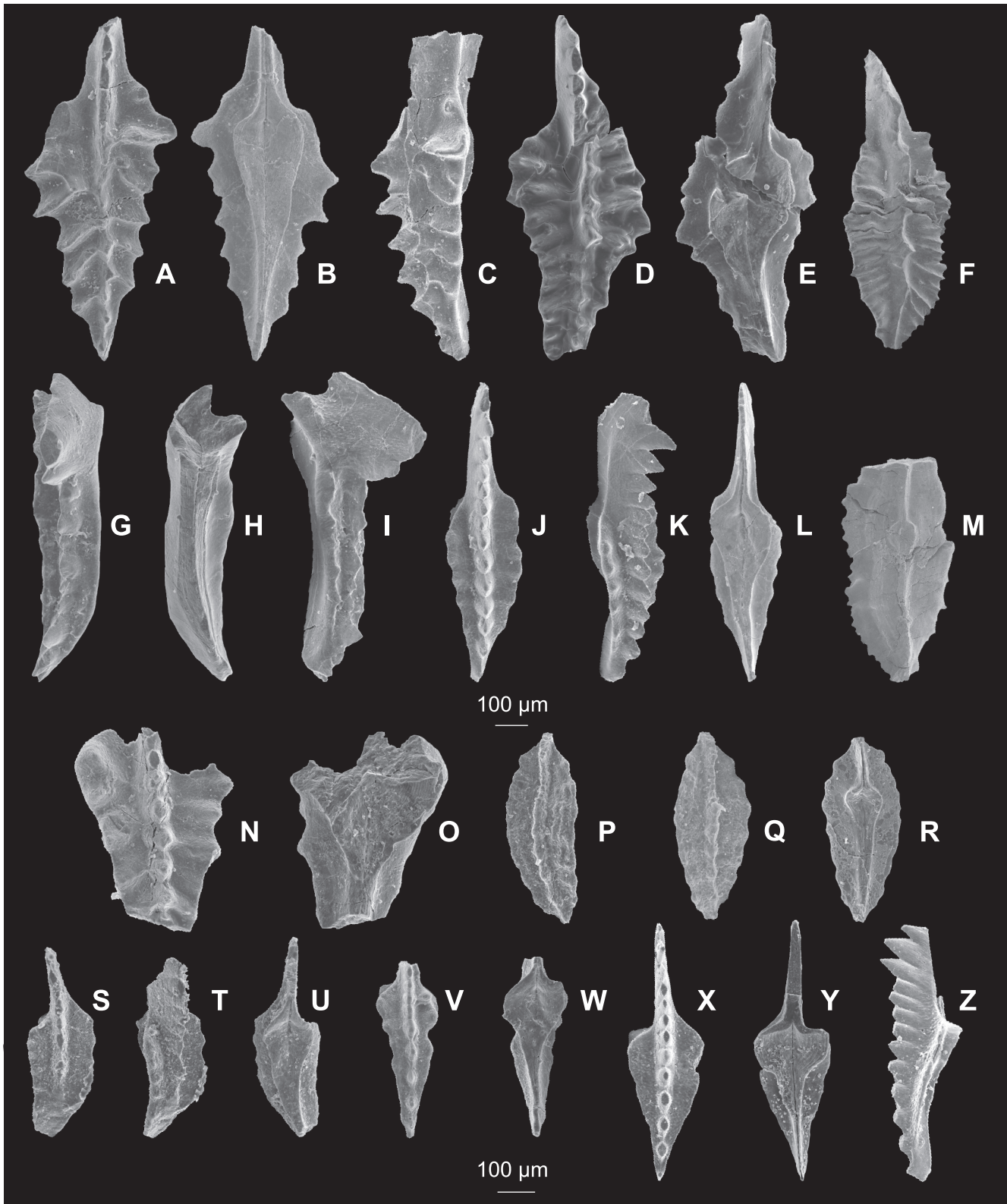


Fig. 8. Selected conodont elements (P₁) of the genus *Pseudopolygnathus* from the Kule section

A–E, N, O – *Pseudopolygnathus primus* Branson and Mehl, 1934a: A–C – upper, lower and lateral views, sample 01A, D, E – upper and lower views, sample 1, N, O – upper and lower views, sample 01A; **F, M, P, R** – *Pseudopolygnathus multistriatus* Mehl and Thomas, 1947: F–M – upper and lower views, sample 1, P, R – upper/oblique, upper and lower views of juvenile stage, sample 8A; **G–I** – genus and species indetermined: G–I – upper, lower and lateral views, sample 1; **J–L** – *Pseudopolygnathus* sp.: J–L – upper, lateral, lower views, sample 01A; **S–U** – *Pseudopolygnathus* cf. *Ps. primus* Branson and Mehl, 1934a: S–U – upper, oblique and lower views of juvenile stage, sample 0; **V, W** – *Pseudopolygnathus fusiformis* Branson and Mehl, 1934a: V, W – upper and lower views of juvenile stage, sample 8A; **X–Z** – *Pseudopolygnathus* cf. *Ps. micropunctatus* Bischoff and Ziegler, 1956: X–Z – upper, lower and lateral views, sample 38; scale bar in all specimens represents 100 μ

taxonomic diversity, composes 55% of the entire assemblage, polygnathids 35%, and pseudopolygnathids 10%. In turn, sample 5B is characterized by the polygnathid-siphonodellid biofacies with 62% of *Polygnathus* and 19% of *Siphonodella*. The 5B sample assemblage is the most abundant and diverse of all studied. In addition to the genera *Polygnathus*, *Siphonodella* and *Pseudopolygnathus*, found also in lower samples, it records the first entry of the bispathodid group including *Bispathodus* and the morphologically similar *Branmehla* and *Mehlina* (Ziegler and Sandberg, 1984). The bispathodid group is third largest in the 5B assemblage, which also contains a single representative of *Protognathodus*.

The bispathodid group continues higher in the section peaking in sample 8A attributable to the polygnathid-bispathodid biofacies. The percentage of *Polygnathus* is 66% and that of bispathodids is 17% while *Pseudopolygnathus* and *Siphonodella* compose 10 and 7%, respectively. The polygnathid-siphonodellid biofacies returns in sample 38, with *Polygnathus* forming 46%, *Siphonodella* 32%, and bispathodids 14% of the whole assemblage.

It is remarkable that *Polygnathus* is dominated by *Po. purus* in all the assemblages investigated. In sample 01A the taxon represents 100% of all polygnathids; in the upper samples 1 and 5B its proportion ranges to ~60%, while in the samples 8A and 38 it attains 66 and 70% of all polygnathids, respectively. Some published interpretations suggest that the subspecies was adapted to environments deeper than shallow-water platforms (Kaiser et al., 2009, 2017; Kalvoda et al., 2015).

The higher proportion and increased diversity of siphonodellids in sample 1 is consistent with the wider trend starting from the *Si. duplicata* Zone (see above). It may have been connected with the eustatic post-Hangenberg rise (Kaiser et al., 2017) and colonization of emptied mesopelagic niches during the transgression (Kalvoda et al., 1999, 2015). A lower proportion of *Siphonodella* is observed higher, in samples 5B and 8A. In the latter assemblage all characteristic earlier-occurring *Siphonodella* species have disappeared, except for *Siphonodella* sp. (transitional form *praesulcata*→*sulcata*). The lack of siphonodellids is not necessarily evidence for shallowing of the Kule Basin, however, as the bispathodid group are characteristic of the euphotic zone of the deep marine environment (Kaiser et al., 2009; Girard et al., 2014; Kalvoda et al., 2015). The revival of *Siphonodella*, associated with the appearance of new species, is observed higher, in sample 38.

The conodont biofacies succession in the Kule section described above is consistent with the universal models noted at the beginning of this chapter. There is a notable lack of the protognathodid-polygnathid biofacies, however, known from other localities of the lower Tournaisian (Kaiser et al., 2009, 2017). This may suggest that the lowermost Tournaisian sample investigated (01A), in which the polygnathid biofacies was found, corresponds to the upper part of the *Pr. kockeli* Zone. Such a supposition is in agreement with the recent data on the DCB in the Kule section, being placed lower than that in Yolkin et al. (2008; see also Fig. 2). The considerable proportion and diversity of *Siphonodella* starting from sample 1 upwards is consistent with the global trend initiated in the *Si. duplicata* Zone. Various proportions of *Siphonodella*, *Polygnathus* and *Bispathodus* in the interval from samples 5B to 38 probably reflect local or regional environmental shifts.

In general, the conodont assemblages analysed from the Kule section, dominated by *Po. purus purus* and accompanying siphonodellids and bispathodids, indicate deep-water marine environments typical of the lower continental slope and rise (Ziegler and Sandberg, 1984; Savoy et al., 1999; Kaiser et al., 2008, 2009, 2017; Kalvoda et al., 2015).

COMPARISON WITH PREVIOUS DATA

The section investigated is here correlated with the previously published log (Yolkin et al., 2008: fig. 14) based on the same location of the DCB, and assuming the same vertical scale (Fig. 2).

The stratigraphic range of the 04F assemblage (*Ps. granulosis* to *Pr. kockeli* zones interval) is wider than but not inconsistent with the range previously attributed to the roughly equivalent samples 96/2 to 96/3, which was placed within an undifferentiated *expansa* Zone (Fig. 2; Erina, 2008a: fig. 14). On the other hand, there is a disparity between the present data on the 01A sample (*kockeli*–*duplicata* zones) and the corresponding 630-3 sample (*praesulcata* Zone; Fig. 2; Erina, 2008a: fig. 14). Consequently, the DCB which was drawn by Yolkin et al. (2008) between their samples 96/4 and 630-4, is located lower in the section, i.e. between the 04F and 01A samples according to our study. Such a lower position has been already suggested by Matyja (2011) and Narkiewicz et al. (2017) and has been detailed by the new data of Erina (fide Salimova 2017, information in an e-mail from December 14th, 2017). The latter author draws the DCB at the base of Bed 5 of Yolkin et al. (2008: fig. 14) corresponding to the central part of our Bed 04, above the position of our sample 04F (Fig. 2).

Also, the present biostratigraphic data from sample 1 (= *Si. jii* Zone; Table 1) differ from that for the slightly higher sample 630-4 (Fig. 2). Yolkin et al. (2008: fig. 14) attributed this sample to the *sulcata* Zone, but from that sample Erina (2008b: pl. 33, fig. 3) illustrated as *Si. angulata* n. sp. an element that actually is a juvenile of *Si. lobata*, which has its first occurrence within the *Si. jii* Zone (Kalvoda et al., 2015; Corradini et al., 2020).

Concerning sample 5B, it is within the undifferentiated *duplicata* Zone according to Yolkin et al. (2008). So, both compared datasets may correspond to each other as the *Si. jii* Zone is equivalent to the former Upper *duplicata* Zone. The same applies for our sample 8A, equivalent to sample 630-10 in the previous study.

Due to the sampling gap we do not have data on the occurrence of the *Siphonodella sandbergi* and *Siphonodella quadruplicata* zones, while our uppermost sample 38 belongs to the undivided *Si. crenulata* Zone. It fits in the interval where this zone was discriminated by Yolkin et al. (2008).

The present results concur with the stratigraphic condensation of the interval around the DCB in the Kule section. This appears to be a universal phenomenon associated with this boundary (e.g., Kalvoda et al., 1999; Kaiser et al., 2009).

SYSTEMATIC PALAEOONTOLOGY

Polygnathus n. sp. A (Fig. 7A–C, H–N)

Description. – Platform is relatively narrow, elongated, nearly symmetrical and curved in the middle part, variously arched in a lateral view. Platform is widest in the anterior part, gradually narrowing posteriorly. In the anterior part the platform margins are more or less parallel but posteriorly the outer margin is curved and parallel to the carina, while the inner one is straight or concave. The anterior platform end is straight whereas the posterior one is slightly rounded. Ornamentation consists of ridges and nodes. Isolated ridges, which may divide into discrete nodes, occur in the most anterior part the platform whereas nodes are present in the remaining part. Nodes tend to be arranged into elongated rows parallel to the carina. Both ridges and nodes are not in contact with the carina.

Carina is quite strongly curved inwards; it reaches the posterior end of the platform. It is accompanied by shallow grooves deepening in the anteriormost part of the platform. It is composed of low nodes in the central and posterior part of the platform, and higher denticles in the anterior part. Rounded, isolated and low nodes (~9) are distributed from 1/3 of the anterior length of the carina to its posterior end. The distance between nodes is larger in the posterior part than in the central one. The nodes are connected by a thin ridge, particularly in the posterior part. In the most anterior part of the platform, nodes are replaced by distinctly higher, narrow, densely situated denticles. There is no distinct boundary between the denticles of the carina and those of the free blade.

The blade is short, composed of 4 to 6 denticles merged at their bases but with free peaks. The denticles are of almost uniform width but of various heights. The first two or three denticles are higher than the remaining ones which are lower, grading into the denticles of the carina. A moderately large basal pit with raised flanges is located in the anterior third of the platform.

Indistinct keel with a furrow extends from the basal cavity to the posterior end of the specimens. The basal cavity with keel is surrounded by a wide crimp with distinct edges.

In the phylogenetically older forms (Fig. 7J, L) the platform and carina are slightly curved inwards. The arc-like bowing in lateral view is lacking. The outer part of the platform may extend farther anteriorly than the inner one. The lower surface of a specimen is nearly flat. The keel is lacking but a distinct furrow extends from the basal cavity to the posterior end.

Material. – Seven specimens from samples 1, 5B and 8A.

Discussion. – The taxon described displays similarities to the specimen from the *sandbergi* Zone figured by Bardashev et al. (2004: pl. 11, figs. 16, 17) as *Eucostapolygnathus* sp. nov. 3. It differs from the latter, however, in the absence of an upturned outer platform margin. In the taxon described both anterior margins are at the same level.

Stratigraphic distribution. – The taxon occurs in the *Si. jii* Zone, and possibly at slightly younger levels.

Genus and species indetermined (Fig. 8G–I)

Description. – The incomplete specimen with a broken anterior part probably belongs to a new taxon (genus ?) distinguished by a high blade, fixed to the right side of the platform. The blade is inclined posteriorwards and consists of two large merged denticles with free (separated) apical parts. The first denticle is considerably higher and almost two times wider than the second one which is connected with a much lower carina.

The platform is very narrow, slightly asymmetrical and its posterior end is twisted inwards. The left anterior part of the platform is wider than the right one. Upper surface is slightly concave. The platform margins are mostly nearly straight, except for the most posterior twisted part, and run parallel to the carina. Small nodes occurring along the margins may merge causing thickening of the margins and a crenulate appearance of the inner margin in side view (Fig. 8G). On the inner side of the platform there are about eight distinct nodes while on the outer side only three weakly developed nodes are observed. Where the blade joins the carina there is a notable constriction of both platform margins (“waistline”). Starting from the constriction, the anterior inner margin is inclined downwards (see Fig. 8I).

Carina is strong, considerably higher than platform margins and extends from its anterior to posterior part. It consists of nine denticles which are wide in side view, of uneven size. They are connected at their bases while their sharp peaks are free. Overall, they are lower posteriorwards, but the highest denticle occurs in the posterior part while, both in front of it and behind it, two small denticles occur.

The development of the basal cavity is unclear as the critical part of the specimen is missing (broken). The lower side is sharply bevelled from keel to platform margins. A high sharp keel with a narrow poorly visible furrow runs from the posterior end of the platform towards its anterior part. More or less in the place of the platform margin constrictions the keel grades into a more clearly visible furrow. Both structures are surrounded by a darker crimp with sharply outlined margins.

Material. – One specimen from sample 1.

Discussion. – The general shape of the element may recall other lower Carboniferous genera characterized by high and short free blades and a narrow platform (*Cavusgnathus*, *Clydagnathus*, *Patrognathus*, *Taphrognathus*), but differs by the presence of the carina above the platform. In fact, all these genera have a distinct medial trough on the platform.

Stratigraphic distribution. – The element comes from the *Si. jii* Zone.

SUMMARY AND CONCLUSIONS

Conodont investigations of the Kule section in SE Uzbekistan document the presence of several zones comprising *Ps. granulosus*–*Pr. kockeli* interval of the uppermost Famennian and the *Pr. kockeli*–*Si. crenulata* interval of the lower–middle Tournaisian. The results of the present conodont study allowed the authors to revise earlier taxonomic and biostratigraphic data (Yolkin et al., 2008; Kim et al., 2008). This revision resulted in placing the position of the Devonian–Carboniferous boundary a few metres lower within the Novchomok Formation relative to the earlier results. A new species of *Polygnathus* has been described in open nomenclature in addition to a peculiar P₁ element reported as genus and species indet., probably constituting a new genus.

The present analysis revealed that the changes in conodont biofacies in the section studied are consistent with the lower Tournaisian biofacies succession generally known from other basins worldwide. The main difference is the absence of the protognathodid–polygnathid biofacies of the middle part of the *Pr. kockeli* Zone, probably corresponding to a lack of adequate data below the lowermost Tournaisian sample investigated. On the other hand, the low frequency of *Siphonodella* and predominance of polygnathids in samples 01A and 0 suggests that the assemblage is older than the *Si. jii* Zone. This would constrain the stratigraphic attribution of the 01A and 0 assemblages to the interval comprising the upper part of *Pr. kockeli* Zone to the *Si. duplicata* Zone. The other difference is the relative abundance of bispathodids which allowed the authors to discern a previously undescribed polygnathid–bispathodid biofacies. The high percentage of *Po. purus purus* and the abundance of siphonodellids and bispathodids are evidence of deep marine environments of the lower continental slope and rise in the Kule part of the sedimentary basin.

Acknowledgements. The authors thank Z. Dubicka (University of Warsaw/University of Silesia, Poland) and M. Rakoński (University of Silesia, Poland) for making available the conodont samples acquired during their fieldwork in Uzbekistan in 2015. This work is a contribution to the project funded by the National Science Centre – Poland (MAESTRO grant 2013/08/A/ST10/00717 to Grzegorz Racki). The study was partly funded by PGI-NRI statutory funds (Project No. 62.9012.1904.00.0). We are grateful to F. Salimova (Stratigraphical Party, SE «Regional GSE», Tashkent, Uzbekistan) for consultations and discussions of the Kule section. Our thanks are extended to the journal reviewers C. Spalletta and T. Kumpan for their constructive comments and suggestions. This study is a contribution to the IGCP Project 652 “Reading geologic time in Palaeozoic sedimentary rocks”.

REFERENCES

- Bardashev, N.P., Bardashev, I.A., Weddige, K., Ziegler, W., 2004.** Stratigraphy and conodonts of the Lower Carboniferous of the Shishkat section (southern Tien Shan, Tajikistan). *Senckenbergiana lethaea*, **84**: 225–301.
- Becker, R.T., Kaiser, S.I., Artz, M., 2016.** Review of chrono-, litho- and biostratigraphy across the global Hangenberg Crisis and Devonian-Carboniferous Boundary. *Geological Society Special Publications*, **423**: 355–386.
- Bischoff, G., Ziegler, W., 1957.** Die Conodontenchronologie des Mitteldevons und des tiefsten Oberdevons. *Abhandlungen des Hessischen Landesamtes für Bodenforschung zu Wiesbaden*, **22**: 1–135.
- Branson, E.R., 1934.** Conodonts from the Hannibal Formation of Missouri. *University Missouri Studies*, **8**: 301–334.
- Branson, E.B., Mehl, M.G., 1934a.** Conodonts from the Bushberg sandstone and equivalent formations of Missouri. *University Missouri Studies*, **8**: 265–299.
- Branson, E.B., Mehl, M.G., 1934b.** Conodonts from the Grassy Creek Shale of Missouri. *University Missouri Studies*, **8**: 171–259.
- Broadhead, T.W., Driese, S.G., Harvey, J.L., 1990.** Gravitational settling of conodont elements: Implications for paleoecologic interpretations of conodont assemblages. *Geology*, **18**: 850–853.
- Bultynck, P., Helsen, S., Haydukiewicz, J., 1998.** Conodont succession and biofacies in upper Frasnian formations (Devonian) from the southern and central parts of the Dinant Synclinorium (Belgium) – (Timing of facies shifting and correlation with late Frasnian events). *Bulletin de l'Institut Royal Sciences Naturelles de Belgique, Sciences de la Terre*, **68**: 25–75.
- Cooper, C.L., 1939.** Conodonts from a Bushberg-Hannibal horizon in Oklahoma. *Journal of Paleontology*, **13**: 379–422.
- Corradini, C., 2008.** Revision of Famennian-Tournaisian (Late Devonian-Early Carboniferous) conodont biostratigraphy of Sardinia, Italy. *Revue de Micropaléontologie*, **51**: 123–132.
- Corradini, C., Barca, S., Spalletta, C., 2003.** Late-Devonian-Early Carboniferous conodonts from the “Clymeniae Limestones” of SE Sardinia (Italy). *Courier Forschungsinstitut Senckenberg*, **245**: 227–253.
- Corradini, C., Kaiser, S.I., Perri, M.C., Spalletta, C., 2011.** *Protognathodus* (Conodonta) and its potential as a tool for defining the Devonian/Carboniferous boundary. *Rivista Italiana di Paleontologia e Stratigrafia*, **117**: 15–28.
- Corradini, C., Schönlaub, H.P., Kaiser S.I., 2017a.** The Devonian/Carboniferous boundary in the Grüne Schneid section. *Berichte des Institutes für Erdwissenschaften, Karl-Franzens-Universität Graz*, **23**: 271–275.
- Corradini, C., Spalletta, C., Mossoni, A., Matyja, H., Over, D.J., 2017b.** Conodonts across the Devonian/Carboniferous boundary: a review and implication for the redefinition of the boundary and a proposal for an updated conodont zonation. *Geological Magazine*, **154**: 888–902.
- Corradini, C., Mossoni, A., Corrigan, M.G., Spalletta, C., 2020.** The Devonian/Carboniferous boundary in Sardinia (Italy). *Palaeobiodiversity and Palaeoenvironments*: 1–8, doi: 10.1007/s12549-019-00411-5
- Dreesen, R. M., 1992.** Conodont biofacies analysis of the Devonian/Carboniferous boundary beds in the Carnic Alps. *Jahrbuch der Geologischen Bundesanstalt*, **135**: 49–56.
- Dreesen, R., Sandberg, C.A., Ziegler, W., 1986.** Review of Late Devonian and early Carboniferous conodont biostratigraphy and biofacies models as applied to the Ardenne shelf. *Annales de la Société Géologique de Belgique*, **109**: 27–42.
- Dubicka, Z., Rakociński, M., 2015.** Raport z wyjazdu terenowego do Uzbekistanu (południowy Tian-Shan), w ramach projektu badawczego NCN MAESTRO “Głębokomorskie środowiska dewonu jako klucz do zrozumienia globalnych perturbacji ekosystemowych” (in Polish) [Report from the fieldwork in Uzbekistan (southern Tien-Shan, in the framework of the NCN MAESTRO Project “Devonian deep-marine environments as a key to understand global ecosystem perturbations” led by prof. dr hab. Grzegorz Rackij]. *Archiwum Instytutu Nauk o Ziemi UŚ, Sosnowiec: GIUS 4-3736.*
- Epstein, A.G., Epstein, J.B., Harris, L.D., 1977.** Conodont Color Alteration – an index to organic metamorphism. *U.S.G.S. Professional Paper*, **995**: 1–27.
- Erina, M.V., 2008a.** Conodonts. In: *Devonian Sequences of the Kitab Reserve Area. Field Excursion Guidebook* (eds. E.A. Yolkin, A.I. Kim and J.A. Talent). International Conference “Global Alignments of Lower Devonian Carbonate and Clastic Sequences” (SDS/IGCP 499 Project joint field meeting), Kitab State Geological Reserve, Uzbekistan, August 25–September 3, 2008, 45. Publishing House of SB RAS, Novosibirsk.
- Erina, M.V., 2008b.** Conodonts. In: *Atlas of the Paleontological Plates. Supplement to a Guidebook of the Field Excursion* (eds. A.I. Kim, M.V. Erina and I.A. Kim). International Conference “Global Alignments of Lower Devonian Carbonate and Clastic Sequences” (SDS/IGCP 499 Project joint field meeting), Kitab State Geological Reserve, Uzbekistan, August 25–September 3, 2008, 45. Tashkent, 2008.
- Flais, G., Feist, R., 1988.** Index conodonts, trilobites and environment of the Devonian-Carboniferous boundary beds at La Serre (Montagne Noire, France). *Courier Forschungsinstitut Senckenberg*, **100**: 53–107.
- Girard, C., Cornée, J.-J., Corradini, C., Fravallo, A., Feist, R., 2014.** Palaeoenvironmental changes at Col des Tribes (Montagne Noire, France), a reference section for the Famennian of north Gondwana-related areas. *Geological Magazine*, **151**: 864–884.
- Hartenfels, S., 2011.** Die globalen *Annulata*-Events und die Dasberg-Krise (Famennium, Oberdevon) in Europa und Nord-Afrika – hochauflösende Conodonten-Stratigraphie, Karbonat-Mikrofazies, Paläoökologie und Paläodiversität. *Münstersche Forschungen zur Geologie und Paläontologie*, **105**: 17–527.
- Hass, W.H., 1959.** Conodonts from the Chappel Limestone of Texas. *U.S.G.S. Professional Paper*, **294**: 365–399.
- Hogancamp, N.J., Stolfus, B.M., Cramer, B.D., Day, J.E., 2019.** A revised conodont zonation of the Tournaisian (Kinderhookian to lower Osagean) and implication for stratigraphic correlation in North America. *Iowa Geological Survey Guidebook*, **30**: 11–17.
- Huddle, J.W., 1934.** Conodonts from the New Albany Shale of Indiana. *Bulletin of American Paleontology*, **21**: 1–136.
- Ji, Q., 1985.** Study on the phylogeny, taxonomy, zonation and biofacies of *Siphonodella* (Conodonta). *Bulletin of the Institute of Geology*, **11**: 51–75.
- Ji, Q., Ziegler, W., 1993.** The Lali section: an excellent reference section for Late Devonian in south China. *Courier Forschungsinstitut Senckenberg*, **157**: 1–183.
- Kaiser, S.I., 2009.** The Devonian/Carboniferous boundary stratotype section (La Serre, France) revisited. *Newsletters on Stratigraphy*, **43**: 195–205.
- Kaiser, S.I., Corradini, C., 2011.** The early Siphonodellids (Conodonta, Late Devonian-Early Carboniferous): overview and taxonomic state. *Neues Jahrbuch für Geologie und Paläontologie Abhandlungen*, **261**: 19–35.
- Kaiser, S.I., Steuber, T., Becker, R.T., 2008.** Environmental change during the Late Famennian and Early Tournaisian (Late Devonian-Early Carboniferous): implications from stable isotopes and conodont biofacies in southern Europe. *Geological Journal*, **43**: 241–260.
- Kaiser, S.I., Becker, R.T., Spalletta, C., Steuber, T., 2009.** High-resolution conodont stratigraphy, biofacies, and extinctions around the Hangenberg Event in pelagic succession from Austria, Italy, and France. *Palaeontographica Americana*, **63**: 97–139.
- Kaiser, S.I., Aretz, M., Becker, R.T., 2016.** The global Hangenberg Crisis (Devonian-Carboniferous transition): review of a first-order mass extinction. *Geological Society Special Publications*, **423**: 387–437.
- Kaiser, S.I., Kumpan, T., Cigler, V., 2017.** New unornamented siphonodellids (Conodonta) of the lower Tournaisian from the

- Rhenish massif and Moravian Karst (Germany and Czech Republic). *Neues Jahrbuch für Geologie und Paläontologie Abhandlungen*, **286**: 1–33.
- Kalvoda, J., Bábek, O., Malovaná, A., 1999.** Sedimentary and biofacies records in calciturbidites at the Devonian-Carboniferous boundary in Moravia (Moravian-Silesian Zone, Middle Europe). *Facies*, **41**: 141–158.
- Kalvoda, J., Kumpan, T., Babek O., 2015.** Upper Famennian and Lower Tournaisian sections of the Moravian Karst (Moravo-Silesian Zone, Czech Republic): a proposed key area for correlation of the conodont and foraminiferal zonations. *Geological Journal*, **50**: 17–38.
- Kim, A.I., Erina, M.V., Kim, I.A., 2008.** Atlas of the paleontological plates. Supplement to a Guidebook of the Field Excursion. International Conference “Global Alignments of Lower Devonian Carbonate and Clastic Sequences” (SDS/IGCP 499 Project joint field meeting), Kitab State Geological Reserve, Uzbekistan, August 25–September 3, 2008, 45. Tashkent, 2008.
- Klapper, G., 1966.** Upper Devonian and lower Mississippian conodont zones in Montana, Wyoming, and South Dakota. *The University of Kansas Paleontological Contributions*, **3**: 1–43.
- Klapper, G., 1971.** *Patrognathus* and *Siphonodella* (Conodonts) from the Kinderhookian (Lower Mississippian) of Western Kansas and Southwestern Nebraska. *Kansas Geological Survey Bulletin*, **202**: 1–14.
- Kumpan, T., Kalvoda, J., Babek, O., Holá, M., Kanický, V., 2019.** Tracing paleoredox conditions across the Devonian-Carboniferous boundary events: a case study from carbonate-dominated settings of Belgium, the Czech Republic, and northern France. *Sedimentary Geology*, **380**: 143–157.
- Matyja, H., 2011.** Membership news. Subcommission on Devonian Stratigraphy SDS Newsletter, **26**: 103.
- Matyja, H., Sobieñ, K., Marynowski, L., Stempień-Satek, M., Małkowski, K., 2015.** The expression of the Hangenberg Event (latest Devonian) in a relatively shallow-marine succession (Pomeranian Basin, Poland): the results of a multi-proxy investigation. *Geological Magazine*, **152**: 400–428.
- Marynowski, L., Zatoń, M., Rakociński, M., Filipiak, P., Kurkiewicz, S., Pearce, T.J., 2012.** Deciphering the upper Famennian Hangenberg Black Shale depositional environments based on multi-proxy record. *Palaeogeography, Palaeoclimatology, Palaeoecology*, **346**: 66–86.
- Mehl, M.G., Thomas, L.A., 1947.** Conodonts from the Fern Glen of Missouri. *Bulletin of the scientific laboratories of Denison University*, **40**: 3–20.
- Mossoni, A., Carta, N., Corradini, C., Spalletta, C., 2015.** Conodonts across the Devonian/Carboniferous boundary in SE Sardinia (Italy). *Bulletin of Geosciences*, **90**: 371–388.
- Narkiewicz, K., Rakociński, M., Corradini, C., Racki, G., 2017.** New conodont data from the Devonian-Carboniferous boundary interval in the Kitab Reserve area (Uzbekistan). *Cuadernos del Museo Geominero*, **22**: 183–185.
- Paschall, O., Carmichael, S.K., Königshof, P., Waters, J.A., Phuong, H.Ta., Komatsu, T., Dombrowski, A., 2019.** The Devonian-Carboniferous boundary in Vietnam: Sustained ocean anoxia with a volcanic trigger for Hangenberg Crises? *Global and Planetary Change*, **175**: 64–81.
- Rakociński, M., Marynowski, L., Pisarzowska, A., Beldowski, J., Siedlewicz, G., Zatoń, M., Perri, M.C., Spalletta, C., Schönlaub, H.P., 2020.** Volcanic related methylmercury poisoning as the possible driver of the end-Devonian Mass Extinction. *Scientific Reports*, **10**: 7344.
- Sandberg, C.A., 1976.** Conodont biofacies of late Devonian *Polygnathus styriacus* Zone in western United States. *Geological Association of Canada, Special Paper*, **15**: 171–186.
- Sandberg, C.A., Ziegler, W., Dreesen, R., Butler, J.L., 1988.** Late Frasnian mass extinction: conodont event stratigraphy, global changes and possible causes. *Courier Forschungsinstitut Senckenberg*, **102**: 263–307.
- Sandberg, C.A., Ziegler, W., Leuteritz, K., Brill, S.M., 1978.** Phylogeny, speciation and zonation of *Siphonodella* (Conodonts, Upper Devonian and Lower Carboniferous). *Newsletters on Stratigraphy*, **7**: 102–120.
- Savoy, L.E., Harris, A.G., Mountjoy, E.W., 1999.** Extension of lithofacies and conodont biofacies models of Late Devonian to Early Carboniferous carbonate ramp and black shale systems, southern Canadian Rocky Mountains. *Canadian Journal of Earth Sciences*, **36**: 1281–1298.
- Shizuya, A., Oba, M., Ando, T., Ogata, Y., Takashima, R., Nishi, H., Komatsu, T., Nguyen, Ph., 2020.** Variations in trace elements, isotopes, and organic geochemistry during the Hangenberg Crisis, Devonian-Carboniferous transition, north-eastern Vietnam. *Island Arc*, **29**, doi: 10.1111/lar.12337.
- Souquet, L., Corradini, C., Girard, C., 2020.** *Siphonodella leiosa* (Conodonts), a new unornamented species from the Tournaisian (lower Carboniferous) of Puech de la Suque (Montagne Noire, France). *Geobios*, **61**: 55–60.
- Spalletta, C., Perri, M.C., Over, D.J., Corradini, C., 2017.** Famennian (Upper Devonian) conodont zonation: revised global standard. *Bulletin of Geosciences*, **92**: 31–57.
- Spalletta, C., Corradini, C., Feist, R., Korn, D., Kumpan, T., Perri, M.C., Pondrelli, M., Venturini, C., 2020.** The Devonian/Carboniferous Boundary in the Carnic Alps (Austria and Italy). *Palaeobiodiversity and Palaeoenvironments*: 1–19, doi: 10.1007/S12549-019-00413-3
- Thompson, T.L., 1967.** Conodont zonation of Lower Osagean rocks (Lower Mississippian) of southwestern Missouri. *Missouri Geological Survey and Water Resources, Report of Investigation*, **39**: 1–88.
- Voges, A., 1959.** Conodonten aus dem Unterkarbon I und II (Gattendorfia- und Pericyclus-Stufe) des Sauerlandes. *Paläontologische Zeitschrift*, **33**: 266–314.
- Yolkin, E.A., Kim, A.I., Weddige, K., Talent, J.A., House, M.R., 1997.** Definition of the Pragian/Emsian Stage boundary. *Episodes*, **20**: 235–240.
- Yolkin, E.A., Kim, A.I., Talent J.A., 2008.** Devonian sequences of the Kitab reserve area. *Field Excursion Guidebook. International Conference “Global Alignments of Lower Devonian Carbonate and Clastic Sequences” (SDS/IGCP 499 Project joint field meeting), Kitab State Geological Reserve, Uzbekistan, August 25 – September 3, 2008, 45. Publishing House of SB RAS, Novosibirsk.*
- Ziegler, W., 1962.** Taxionomie und Phylogenie Oberdevonischer Conodonten und ihre stratigraphische Bedeutung. *Abhandlungen des Hessischen Landesamtes für Bodenforschung zu Wiesbaden*, **38**: 1–166.
- Ziegler, W., Sandberg, C.A., 1984.** *Palmatolepis*-based revision of upper part of standard Late Devonian conodont zonation. *GSA Special Papers*, **196**: 179–194.
- Ziegler, W., Sandberg, C.A., 1990.** The Late Devonian standard conodont zonation. *Courier Forschungsinstitut Senckenberg*, **121**: 1–115.
- Ziegler, W., Sandberg, C.A., 1996.** Reflexions on Frasnian and Famennian Stage boundary decisions as a guide to future deliberations. *Newsletters on Stratigraphy*, **33**: 157–80.